Sustainable Cities and Society 72 (2021) 103045

Contents lists available at ScienceDirect

Sustainable Cities and Society

journal homepage: www.elsevier.com/locate/scs

Influence of urban morphological characteristics on thermal environment

Jun Yang [a,b,*], Yuxin Yang [c], Dongqi Sun [d,*], Cui Jin [a], Xiangming Xiao [e]

[a] Human Settlements Research Center, Liaoning Normal University, Dalian, 116029, China
[b] Jangho Architecture College, Northeastern University, Shenyang, 110169, China
[c] Human Settlements Research Center, Liaoning Normal University, 116029, Dalian, China
[d] Key Laboratory of Regional Sustainable Development Modeling, Institute of Geographic Sciences and Natural Resources Research, CAS, Beijing, 100101, China
[e] Department of Microbiology and Plant Biology, Center for Spatial Analysis, University of Oklahoma, Norman, OK, 73019, USA

ARTICLE INFO

Keywords:
Urban morphological characteristics
Thermal environment
Numerical simulation
Dalian

ABSTRACT

Variation in urban microclimate is closely related to the three-dimensional characteristics of cities. To reveal the influence of urban spatial forms on land surface temperature (LST), the spatial distribution of LST and five urban morphology indicators were analyzed, namely floor area ratio (FAR), plot ratio (PR), absolute rugosity (R_a), mean aspect ratio (λ_c), and sky view factor (SVF). Based on correlation analysis and numerical simulations, the influence of three-dimensional characteristics on the urban thermal environment of Dalian, China was then analyzed. The results showed that in Dalian, LST ranged from 23.2–50.7 °C, and Moran's I was 0.94, indicating that LST presents a strong spatial positive correlation. The buildings in the study area were mainly multi-story and high-rise buildings and mostly distributed in a medium-density area. LST exhibited the highest positive correlation (correlation coefficient = 0.569) with FAR and was negatively correlated with SVF (correlation coefficient =−0.270). The simulation results showed that in the medium density range (FAR <0.6), an increase in FAR changed the wind speed, thereby affecting the urban thermal environment. The results demonstrate the influence of urban morphology on the thermal environment and provide scientific ideas for future planning and construction of "cool cities".

1. Introduction

In recent years, under global warming and rapid urbanization, urban populations have surged, and anthropogenic factors have exerted a significant impact on the urban thermal environment, resulting in the urban heat island (UHI) effect (Feng, Wang, Jin, & Yang, 2019; Jiang, Zhan, Yang, Liu, & Huang, 2020; Qiao, Huang, Xu, Sun, & Wu, 2019; Qiao, Sun, Sun, Xu, & Yang, 2019; Zhai, Yuan, Yu, & Guo, 2019). The UHI effect directly affects the quality of the urban living environment and public health, but also has a far-reaching impact on urban energy consumption and sustainable development of cities, which can increase the risk to urban security (Kuang, 2018; Qiao, Huang et al., 2019; Qiao, Sun et al., 2019; Yao, Chen, & Qian, 2018, Zhou & Tian, 2020).

With the continuous development of social economy, rapid urbanization has become inevitable on a global scale. As a large number of people now reside in cities, these continue to expand, while the available land resources continue to decrease, thereby resulting in a continuous increase in the number of high-rise and super-high-rise urban buildings, especially in developing countries (Fan, Yue, Zhang, Huang, & Messina, 2020; Yue, Zhang, & Liu, 2016; Yue, Liu, Zhou, & Liu, 2019). The three-dimensional characteristics of a city are related to the urban canopy and the scale of streets and buildings and directly affect human thermal sensations. These characteristics can have a significant impact on outdoor climatic conditions, building energy balance, and pollutant diffusion (Salata, Golasi, Vollaro, & Vollaro, 2015; Yang, Niyogi, Tewari, Aliaga, & Chen, 2016; Yu, Chen, & Wong, 2020). The three-dimensional urban morphology affects the urban microclimate by changing the urban surface structure and local ventilation patterns (He, Ding, & Prasad, 2020; He, Ding, & Prasad, 2020; Luo, Yang, Sun, & He, 2021; Ren, Yang, Cheng, Xing, & Fang, 2018; Ren, Cai, Li, Shi, & Linda, 2020; Sun, Liu, Wang, Wang, & Che, 2020; Zhang, Li, Wu, Lin, & Chu, 2020; Zhao, Shen, Li, Wang, & He, 2020). Increasing global temperatures have increased the frequency of extreme weather events. As the most densely populated region, cities also form the centers of global economic growth. Therefore, the sustainable development of urban construction is the focus of human social development. The C40 Cities Climate

* Corresponding authors.
E-mail addresses: yangjun8@mail.neu.edu.cn (J. Yang), 15998620818@139.com (Y. Yang), sundq@igsnrr.ac.cn (D. Sun), cuijin@lnnu.edu.cn (C. Jin), xiangming.xiao@ou.edu (X. Xiao).

https://doi.org/10.1016/j.scs.2021.103045
Received 2 March 2021; Received in revised form 20 May 2021; Accepted 22 May 2021
Available online 27 May 2021
2210-6707/

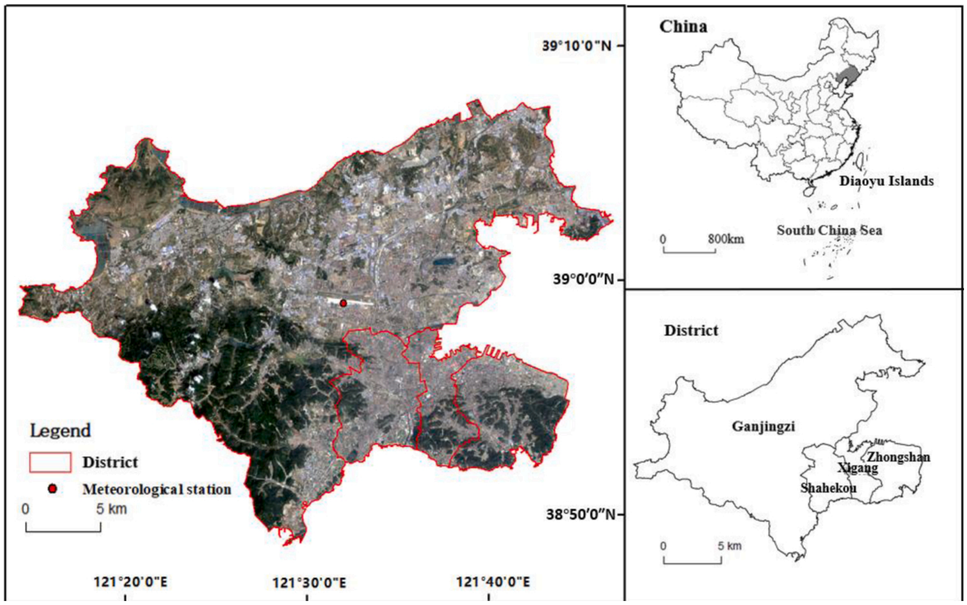

Fig. 1. Location of the study area.

Leadership Group (C40) noted in the ‘Urban Climate Action Impacts Framework’ that cities must be at the forefront of efforts to avoid the worst of climate change, as they will bear the brunt of its effects (C40 cities, 2018). In partnership with C40, the McKinsey Centre for Business and Environment has published ‘Focused Acceleration: A strategic approach to climate action in cities to 2030’. This report lists more than 450 emission-reducing actions, half of which are directly related to buildings (C40 China Buildings Programme, 2018; McKinsey, 2017). In order to achieve sustainable urban development, many scholars have proposed the concept of "cool cities." Studies have demonstrated that the main method of alleviating the UHI effect is to reduce the surface temperature of buildings and urban spaces. This includes creating cooler urban surfaces (roofs and sidewalks, etc.) and improving the urban architectural form and layout. Promoting green infrastructure in urban construction (trees, parks, forests and green roofs) can also achieve local cooling and alleviate UHI effects (Antonio, Federica, Raffaele, & Francesca, 2020; Farshid, Ester, Ebrahim, & Soran, 2019; He, 2019; Kibria, Timothy, Jedediah, & OhJin, 2016; Santamouris & Young Yun, 2020; Yue et al., 2019). At present, two-thirds of China’s building stock is located in cities; this figure has been predicted to reach 80 % by 2050 (C40 China Buildings Programme (C40 CBP, 2018). Therefore, focusing on urban construction issues is essential to alleviate the UHI effect and improve the living environment of residents.

Changes to the urban morphology and microclimate (surface and air temperature), caused by the continuous expansion of urban buildings in both the horizontal and vertical directions, have a significant impact on the health and comfort level of urban residents. Therefore, research has focused on the relationship between urban three-dimensional morphology and urban thermal environment (Yang et al., 2021; Yang, Shi, Xia, Xue, & Cao, 2020; Yang, Wang, Xiu, Xiao, & Xia, 2020; Yang, Sun, Ge, & Li, 2017). Surface temperature can be retrieved from a wide range of remote sensing images; thus, most studies have focused on the correlation between urban morphological characteristics and surface temperature. Current research on the relationship between urban three-dimensional morphology and land surface temperatures adopts two types of analysis: (1) statistical analysis (i.e., correlation analysis, multiple regression, and other statistical methods) is used to analyze the influence of urban morphology indicators on the land surface temperature (Mahanta & Samuel, 2020; Meng & Xiao, 2018; Wang, Cot, Adolphe, Geoffroy, & Sun, 2017; Wang, Liang, Yang, Liu, & Su, 2017; Zhang & Cheng, 2019); and (2) numerical simulations, which are used to simulate and visualize the changes in temperature, wind speed, average radiation temperature, and other parameters over a small area using simulation software, which can more accurately reflect the influence of climate change and urban morphology updates on urban microclimates (Zhou & Tian, 2020). Many scholars have used the “local climate zone” (LCZ) classification system (Stewart & Oke, 2012; Stewart, Oke, & Krayenhoff, 2014), selecting the urban morphology indicators closely related to the urban thermal environment, such as building density, building height, plot ratio (PR), sky view factor (SVF), frontal area index, and other parameters, to analyze the morphology of urban organization. By exploring the influence of urban morphology on thermal environment indices, namely surface temperature and wind potential, the correlation between the two parameters has been analyzed to further explore the influence of a specific urban morphology on environmental temperature (Su, Lv, & Yang, 2018; Wang, Cot et al., 2017, Wang, Liang et al., 2017; Wei, Song, Wong, & Martin, 2016; Yan, Su, & Guan, 2019; Yang, Su, Xia, Jin, & Li, 2018; Yang, Jin, Xiao, Jin, & Xia, 2019; Yang, Wang, Xiao, Jin, & Xia, 2019). Other studies have considered the relationship between different local urban forms and the thermal environment as the starting point to explore their relationship through numerical simulations (Galal, Sailor, & Mahmoud, 2020; Liu, Li, Yang, Mu, & Zhang, 2020; Toparlar, Blocken, Maiheu, & van Heijst, 2017) and have illustrated the complex interactions between three-dimensional morphological characteristics and the local thermal environment in urban settings (Allegrini, Dorer, & Carmeliet, 2015; Wang, Cot et al., 2017, Wang, Liang et al., 2017). Some studies have determined the factors affecting the urban thermal environment under a specific layout by analyzing the correlation between typical characterization parameters (such as building height, building density etc.) under different building layouts and simulation results (Wang, Zhou, Wang, Fang, & Yuan, 2018; Yang, Shi et al., 2020; Yang, Wang et al., 2020; Yu et al., 2020). Other studies have focused on the temperature, humidity, wind speed, average radiation temperature and predicted mean vote (PMV) generated in the simulations to explore the influence of urban geometric structure and spatial layout on the thermal environment (Antoniou, Montazeri, Neophytou, & Blocken, 2019; Huang, Tsai, & Chen, 2020; Wang, Cot et al., 2017, Wang, Liang et al., 2017). The results from all of these studies have demonstrated that a single index is insufficient for measuring the direct relationship between urban morphology and the thermal environment; temperature change is often related to a variety of urban morphological characteristics. It was also observed that

Table 1
Data sources and descriptions.

Data	Descriptions	Source	Sample
Remoting Sensing data	Landsat8 OLI (30 m) Landsat8 TIRS (100 m) 2018-8-9	USGS, earthexplorer.usgs.gov	
Building data	Building outline, height, floor and types. 2018	Baidumap, map.baidu.com	
Meteorological data	2018-8-9	China Meteorological Data Network, rp5.ru	–

Table 2
Building height classification.

Building type	Classification standard/floor
Low-rise building	1−3
Multistory building	4−6
Middle-high rise building	7−9
High-rise building	10−39
Super-High rise building	> = 40

three-dimensional morphological characteristics have a more significant impact on the urban thermal environment than two-dimensional characteristics (Huang & Chen, 2020; Ku & Tsai, 2020; Li, Ren, & Zhan, 2020; Tian, Zhou, Qian, Zheng, & Yan, 2019). Therefore, it is necessary to select indices closely related to the three-dimensional characteristics of cities and combine them with statistical analysis and numerical simulation to explore the influence of urban morphology on the urban thermal environment, based on correlation analysis.

This study analyzed the spatial relationship between the thermal environment and three-dimensional architectural form of urban settings, by using morphological indicators to determine the architectural parameters that have the greatest impact on surface temperature in Dalian, China. Subsequently, the software ENVI-met was used to simulate the thermal environment of the research area to determine the details of the deep connection between urban morphology and the urban thermal environment. Thus, this study aims to improve our understanding of the causes of UHIs in specific environments.

2. Data and methods

2.1. Study area

Dalian is located between 121°44'–121°49' E and 39°01'–39°04' N at the southernmost point of the Liaodong Peninsula in northeastern China, in the East Asian monsoon region. It has a mild climate which features four distinct seasons, humid air, concentrated precipitation, and strong winds. In this study, the Zhongshan, Xigang, Shahekou, and Ganjingzi Districts were selected as study sites (Fig. 1).

2.2. Research data

The urban morphology parameters were calculated using the building data of Dalian. Land surface temperatures were retrieved from Landsat8 remote sensing image data (August 9, 2018, cloud content of less than 5 %). The historical meteorological data on August 9, 2018 were selected as the initial conditions for the numerical simulation (Table 1). The building data contain information such as the basic height of the building, the number of floors, the footprint, and the perimeter. Urban morphology indicators were calculated using geographical information systems (GIS). The buildings in the study area were categorized according to the current national 'Code for Design of Civil Buildings' (GB50352-2005; (China, 2015) (Table 2). The images were first preprocessed in ENVI 5.3 using the FLAASH atmospheric correction module to eliminate the influence of the atmosphere and sun on the reflection information and to obtain accurate surface reflection information. The Mono-window algorithm was used to calculate the surface

Table 3
Description of urban morphology indicators.

Urban morphological indicator	Formula and Description
Floor area ratio (FAR) Floor area ratio, also called building coverage ratio or building density, is defined as the ratio of footprint of the buildings to the overall site area.	$FAR = \lambda_p = \sum_i A_i/S$ where Ai is the build area of the ground floor of the ith building, S represents the total area of the land. The building coverage ratio is an indicator to describe the building density and the land use.
Plot ratio(PR) Plot ratio, also called land use coefficient, is defined as the amount of construction permitted (in planning) on a land according to its size.	$PR = \lambda_a = \sum_{ij}(A_{ij})/S$ where Aij is the built area of the jth floor of the ith building and S represents the total area of land.
Mean aspect ratio(λc) The indicator provides extra information on the links between building surfaces and the external environment in relation to the ground surface.	$\lambda_c = \sum_i E_i/S$ where Ei is the envelop area of the ith building, which includes the surfaces of all the external walls and the roofs.
Absolute rugosity(R_a) As a parameter to describe the roughness of a surface to resist the free wind, absolute rugosity for a city is the average obstacle height over the whole examined area.	$R_a = \sum_i (A_i N_i)\Delta H/S = \overline{H} * \lambda_p$ Where Ni is the number of floors of the ith building,ΔH is the average height of a building.
Sky view factor(SVF) SVF is defined as the ratio of the amount of radiation received (or emitted) on the surface of the earth to the amount emitted (or received) by the entire hemisphere and is used to measure the extent to which radiation transmission at a particular location is blocked. SVF = 0 means the sky is obstructed so that all radiation is blocked; SVF = 1 means there is no obstruction and the earth receives (or emits) all radiation.	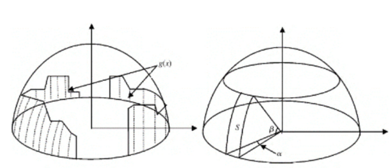 $SVF = 1 - \sum_{i=0}^{n} \sin^2\beta \cdot \left(\frac{\alpha}{360}\right)$ where n = 360/α.

Table 4
Model parameters.

Models		
 FAR = 0.18 (a)	 FAR = 0.36 (b)	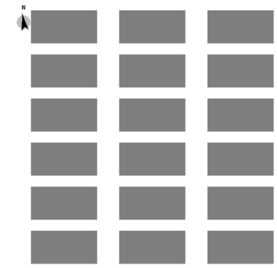 FAR = 0.54 (c)

temperature (Qin, Zhang, Karnieli, & Berliner, 2001). Landsat thermal infrared band 10 was used to retrieve the LST through the following formulas:

$$T_s = (a(1 - C - D) + (b(1 - C - D) + C + D)T_{10} - DT_a)/(C - 237.15) \quad (1)$$

$$C = \varepsilon\tau \quad (2)$$

$$D = (1 - \tau)[1 + (1 - \varepsilon)\tau] \quad (3)$$

Here, Ts is the retrieved LST (K); T10 is the brightness temperature (K) on the sensor; Ta is the average temperature of the atmosphere (K); a and b are reference coefficients (a = −67.355351, b = 0.458606); ε is the land surface emissivity of T10; and τ is the atmospheric transmittance of T10.

Table 5
Initial conditions of the simulation.

Data type	Parameter	Value
Simulation time	Date	2018-08-09
	Time	24 h
Meteorological parameters	Wind speed	3.0 m/s
	Wind direction	135 °
	Minimum air temperature	25.7 °C
	Maximum air temperature	30.7 °C
	Minimum relative humidity	57.00 %
	Maximum relative humidity	83.00 %

2.3. Research methods

Firstly, the spatial distribution of the surface temperature in summer was analyzed, and five urban form indicators, namely floor area ratio (FAR), plot ratio (PR), absolute rugosity (Ra), mean aspect ratio (λc), and sky view factor (SVF), were selected for calculation and visualization. The correlation between the land surface temperature and urban morphology parameters was then calculated to obtain the indicators with the greatest influence on the surface temperature. This indicator was then set as the only variable. Under the premise of only controlling the change in this indicator, the urban buildings were simplified and modeled through ENVI-met to explore the influence of this indicator on the variables that make up the urban thermal environment, such as temperature, wind speed, relative humidity, and mean radiant temperature. Preprocessing of images, including radiometric calibration and FLAASH atmospheric correction, was performed in ENVI 5.3. The indicators were calculated using ArcGIS 10.2, Pearson correlation analysis was performed using SPSS 24.0, and ENVI-met 4.4 was used for numerical simulation.

2.3.1. Urban morphology indicators

Urban morphology is connected to the urban canopy and the scale of streets and buildings, and can significantly affect the wind patterns in urban areas and thereby affect human thermal sensation. Therefore, the urban morphological indicators listed in Table 3 were selected to analyze the effect of architectural forms on urban surface temperature (Wang, Cot et al., 2017, Wang, Liang et al., 2017).

2.3.2. Correlation analysis

The Pearson's simple correlation coefficient *r* was used to calculate the correlations between parameters:

$$r = \frac{\sum (x - \bar{x})(y - \bar{y})}{\sqrt{\sum (x - \bar{x})^2 \sum (y - \bar{y})^2}} \quad (4)$$

where (x, y) and $(\bar{x}, \bar{y})$ are the observed and average values of variables x and y, respectively.

2.3.3. Numerical simulation

The microclimate simulation software ENVI-met was developed in 1998 by Michael Bruce and Heribert Fleer of the University of Bochum, Germany (Yang, Shi et al., 2020; Yang, Wang et al., 2020). This software simulates the urban microclimate based on computational fluid dynamics, fundamental laws of thermodynamics, and theoretical knowledge of urban meteorology (Abdallah, Hussein, & Nayel, 2020; Sharmin, Steemers, & Matzarakis, 2017; Tsoka, Tsikaloudaki, & Theodosiou, 2018; Tsoka, Tsikaloudaki, & Theodosiou, 2018). It provides a spatial precision of 0.5–10 m and a temporal precision of 10 s, and the typical simulation duration is 24–48 h. Such simulations provide accurate reflections of the impact of microclimate change and urban landscape renewal on the microclimate of the study are. The version used in this study was ENVI-met 4.4.

Considering the accuracy and scientific nature of the simulation, the simulation scale was set to 100 m × 100 m. To ensure that other parameters (building height, layout, etc.) were not changed and that building density was the only variable factor, the urban building model was simplified. The dimensions of each building model were set based on the GIS calculation results, as 20 m × 15 m × 15 m. The specific model parameters are presented in Table 4 and the initial conditions of the simulation are shown in Table 5. Combining the calculation results of this paper and the building density classification standard from the research of Yang et al. (2017), three density grades of 0.18, 0.36 and 0.54 were used to explore the specific influence of building density on the four thermal environment representational variables, namely, air temperature, wind speed, relative humidity, and mean radiation temperature.

In the thermal environment simulation, there was a slight deviation between the actual measured temperatures and the simulated temper-

Table 6
The statistical results of surface temperature in different regions (℃).

District /Value	Minimum	Maximum	Range	Average	Standard deviation
Ganjingzi District	23.28	49.01	25.73	34.82	3.29
Shahekou District	27.40	47.02	19.62	36.62	2.88
Xigang District	28.13	50.73	22.60	36.90	3.40
Zhongshan District	25.50	43.87	18.37	34.99	2.88

atures. In this study, percentage error (PE), root mean square error (RMSE), and R^2 were used to evaluate the accuracy of the simulation.

$$PE = \frac{|a - b|}{a} \times 100\% \quad (5)$$

where ‘a’ denotes a measured value and ‘b’ denotes a simulated value.

$$RMSE = \sqrt{\frac{1}{N}\sum_{t=1}^{N}(a_t - b_t)} \quad (6)$$

where ‘a’ denotes a measured value, ‘b’ a simulated value, and ‘N’ the number of measurements.

3. Results and analysis

3.1. Spatial distribution of surface temperature and urban morphology

The distribution of buildings in the study area is shown in Fig. 3. The buildings are mostly situated in the eastern part of the study area and are taller here. Conversely, buildings in the western region are more sparsely distributed and lower in height. Table 6 shows that the surface temperature in the study area ranged from 23.2–50.7 °C, with an average temperature difference of 2.08 °C. The highest temperature was measured in Xigang District (50.73 °C, highest average temperature of 36.90 °C), while the lowest temperature of 23.28 °C was measured in

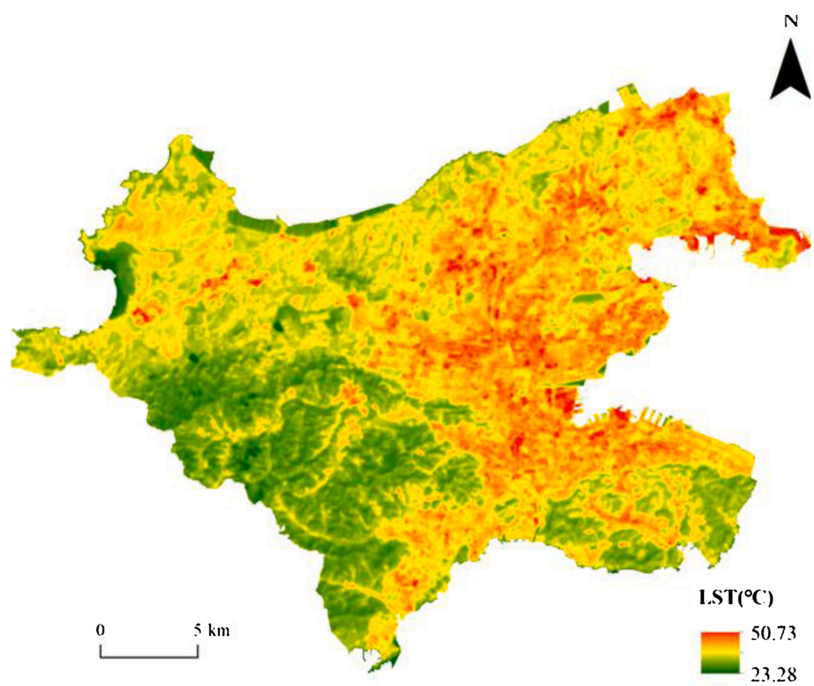

Fig. 2. The spatial distribution of land surface temperature in the study area.

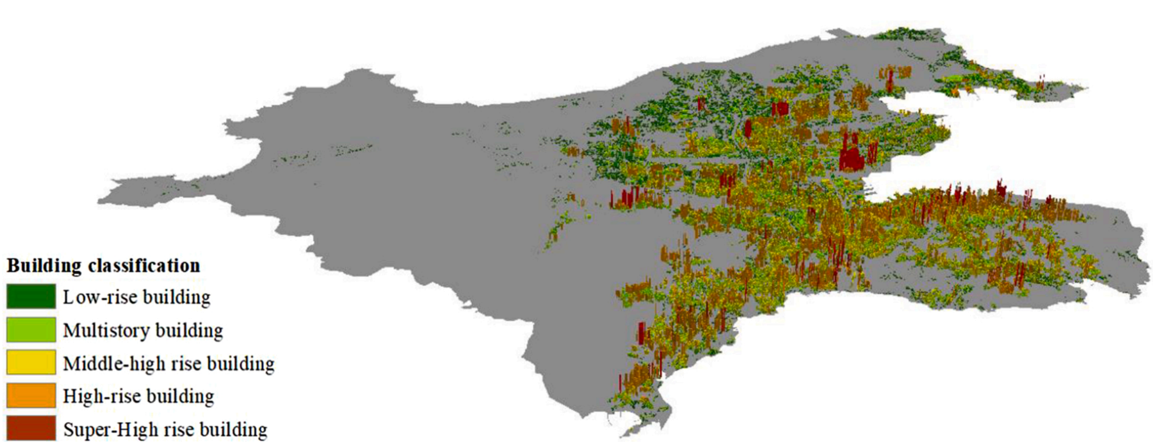

Fig. 3. 3D display of building data.

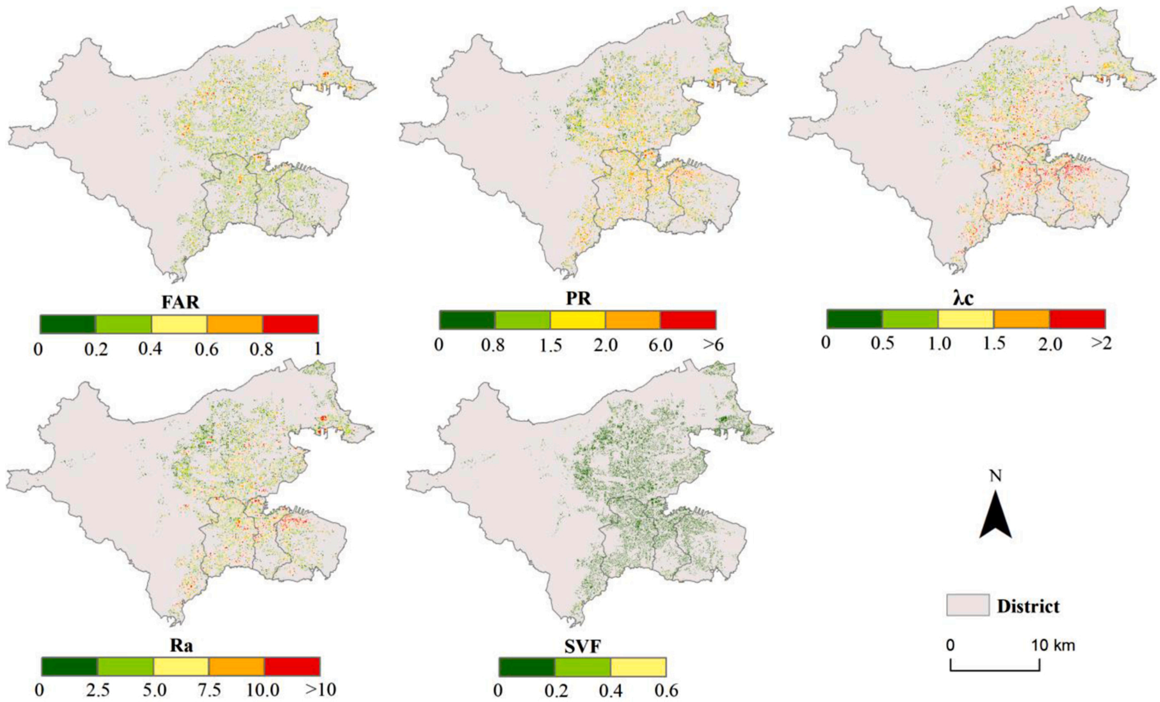

Fig. 4. The spatial distribution of urban morphological parameters.

Table 7
The statistical results of building stock in different regions.

District	Low-rise	Multistory	Middle-high rise	High-rise	Super-high rise
Ganjingzi District	54.81 %	23.47 %	12.75 %	8.50 %	0.47 %
Shahekou District	25.15 %	31.08 %	28.37 %	14.90 %	0.50 %
Xigang District	33.25 %	30.94 %	24.88 %	10.88 %	0.05 %
Zhongshan District	30.01 %	30.81 %	22.42 %	15.77 %	0.98 %
Total	44.45 %	26.45 %	17.86 %	10.75 %	0.50 %

Ganjingzi District. The spatial autocorrelation analysis of the surface temperature revealed that the global spatial autocorrelation coefficient (Moran's I) had a value of 0.94, indicating that the surface temperature exhibits a strong positive spatial correlation. Fig. 2 shows that the northeast of the study area is the high-temperature region, whereas the southwest generally exhibited lower temperatures, which is consistent with the spatial distribution of buildings. This result can be explained by the concentration of buildings, dense population, and low vegetation coverage in the northeastern part of the study area, which increases the surface temperature, whereas the southwest and southeast of the study area contain large green spaces and nature reserves with limited building coverage, resulting in relatively low surface temperatures.

Fig. 4 shows that buildings are mainly distributed in the eastern part of the study area, with the building density ranging between 0.2 and 0.6, indicating a medium-density area. PR values of <0.8 indicate low-rise buildings, PR of 0.8–1.5 indicates normal multi-story buildings, PR of 1.5–2.0 indicates multi-story and high-rise buildings, PR of 2.0–6.0 indicates high-rise buildings, and PR > 6.0 indicates super high-rise buildings. Roughness reflects the vertical characteristics of urban buildings and represents the average obstacle height of the measured area. Table 7 shows that with the exception of Ganjingzi District, about 70 % of the buildings in the study area are multi-story and high-rise buildings, which is consistent with the trend exhibited in Fig. 3, where most regions have PR values of >2 and Ra values of >6 m. The λc value is influenced by the horizontal and vertical dimensions of the buildings; thus, it plays an important role in heat exchange between the buildings and the environment. The high values of these four indicators (FAR, PR, Ra, λc) are mostly distributed in the Zhongshan and Xigang Districts because the area around the Qingniwa Bridge and Renmin Road in the north of Zhongshan District is the most prosperous commercial, financial, and information center in Dalian, with a large number of high-rise office buildings and shopping malls. The total land area of Xigang District is relatively small, as is the available land area. However, continuous expansion of the urban population and urban areas have caused a significant increase in building density and building height in the region. SVF ranges from 0.0 to 0.6 and is in the range of 0.0–0.4, indicating that the buildings have a stronger shielding effect on solar radiation. The higher the building height and density, the smaller the SVF in the area, i.e., the stronger the shielding effect on solar radiation.

3.2. Analysis of correlation between LST and urban morphology

The linear fitting results show that the correlation coefficients between the surface temperature and FAR, PR, Ra, λc, and SVF were 0.569, 0.446, 0.429, 0.463, and -0.270, respectively, all significant at the level of 0.01 (Table 8). Consistent with the linear fitting results, as FAR, PR,

Table 8
The correlation between land surface temperature and urban morphological parameters.

	FAR	PR	R_a	λ_c	SVF
LST	0.569**	0.446**	0.429**	0.463**	−0.270**

** indicates significant correlation at 0.01 level (double tails).

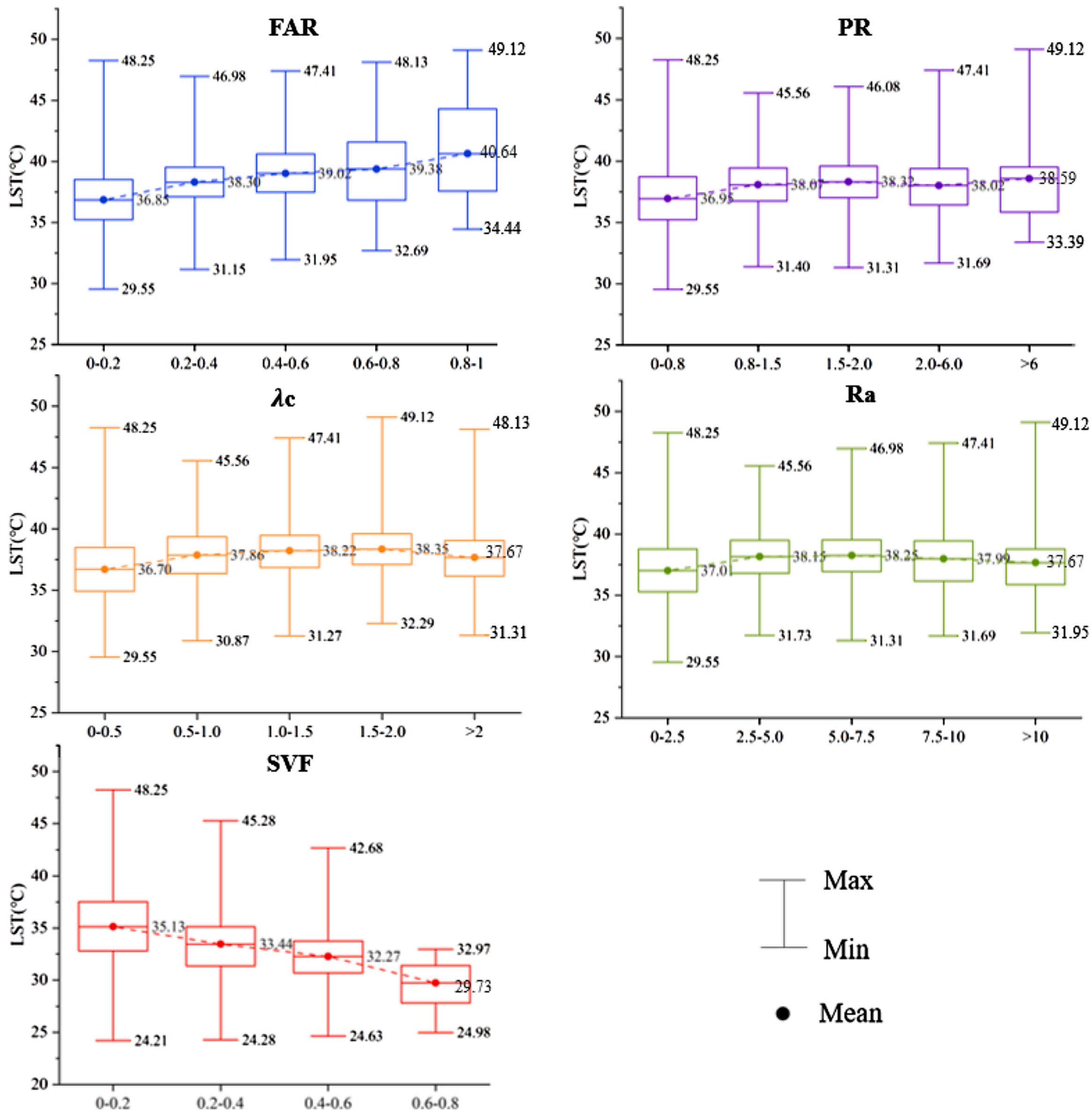

Fig. 5. The analysis results of the distribution interval between morphological parameters and land surface temperature.

Ra, and λc increased, the average surface temperature in each interval also increased (Fig. 5). With a horizontal increase in building distribution and a vertical increase in building height, the surface area of the buildings receiving solar radiation will also increase. This results in the lengthening of the heat radiation process between the buildings, and a reduction in air circulation, which is not conducive to the dissipation of heat; thus, the land surface temperature will rise. The maximum value of the land surface temperature initially decreased and then increased, and the minimum values generally showed an upward trend. The SVF was negatively correlated with the land surface temperature; thus, as SVF increased, the average land surface temperature gradually decreased.

3.3. Simulation results

To ensure the reliability of the simulation, the results were compared with data from a local meteorological station located in Dalian at Zhoushuizi Airport (China Meteorological Data Network) (Fig. 6). The minimum PE of the temperature was 1.26 %, the maximum PE of the temperature was 6.29 %, and the average statistical error was 3.90 %, with RMSE = 1.23 °C and R^2 = 0.870. Referring to the range of simulation accuracy in Table 9, the overall value was within its error range, indicating that the simulation results are relatively reliable.

In the results of simulations with different building densities, the three curves of relative humidity variation coincide, the air temperature and mean radiation temperature exhibit slight differences, and only the wind speed is significantly affected by building density (Fig. 8). Fig. 7 shows the spatial distribution of the three models and illustrates differences in air temperature, wind speed, relative humidity, and mean radiation temperature at 14:00 between each model. The increase in building density causes a gradual decrease in building spacing, which changes the street aspect ratio to a certain extent. This in turn blocks the airflow between the buildings, reducing the ventilation and heat dissipation in the building group, resulting in a decline in wind speed. The wind speed is only higher at the tuyere; the higher the building density, the smaller the high-wind-speed area and the larger the proportion of the low-wind-speed area, which leads to poor ventilation and thermal discomfort. According to Fig. 9, the 24 h average wind speeds from models a, b, and c (where a, b, and c represent FARs of 0.18,0.36 and 0.54, respectively) were 1.48, 1.79, and 2.97 m/s, respectively. When FAR increased from 0.18 to 0.36, the average rate of change in the wind

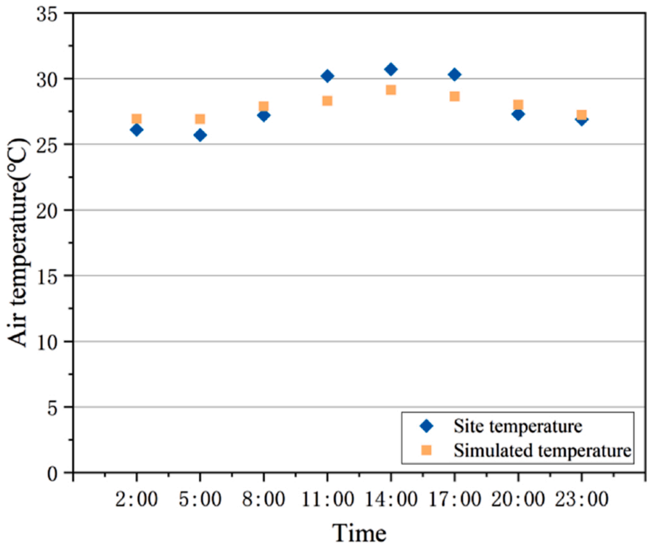

Fig. 6. The comparison of site temperature and simulated temperature.

Table 9
Verification of simulation accuracy.

Verification method	Error range
Percentage Error	3.75 %
RMSE	1.11−1.62℃
R^2	>0.8

speed was 15.76 %, when FAR increased from 0.36 to 0.54, it was 65.92 %, and when FAR increased from 0.18 to 0.54, it was 92.12 %. This indicates that with a medium building density (FAR < 0.6), the wind speed tends to increase with the increase in building density.

4. Discussion

Rapid urbanization intensifies the UHI effect, which not only poses a threat to the sustainable development of cities and affects human health, but also brings huge economic and social losses. To reduce the damage caused by the UHI effect, some scholars have proposed the concept of "cool cities", in which the local thermal environment is improved by optimizing the building layout. Therefore, this study investigated the influence of the three-dimensional morphological characteristics of a city on the local thermal environment, and by using numerical simulations, revealed the influence of urban buildings on the surrounding thermal environment. The results will improve our understanding of the influence of urban morphology on the variations in the urban thermal environment and will support future urban planning and construction efforts to realize sustainable urban development.

4.1. Selection of parameters

Most studies on the correlation between urban morphology and land surface temperature have selected two-dimensional or three-dimensional indicators and examined them separately: a common two-dimensional indicator is building density (Berger, Rosentreter, Voltersen, Baumgart, & Schmullius, 2017; Yang et al., 2018); three-dimensional indicators include building height, PR, and SVF (Guo, Han, Xie, Cai, & Zhao, 2020; Li et al., 2020; Yang, Shi et al., 2020; Yang, Wang et al., 2020). In this study, where the effects of both two-dimensional and three-dimensional factors were considered, λc and Ra were also introduced. These two indicators can characterize the three-dimensional morphology of the city, and also have a degree of influence on the local ventilation effect and the heat exchange between urban buildings and the environment (Wang, Cot et al., 2017, Wang, Liang et al., 2017). Therefore, it is more scientifically meaningful to study the correlation between these and the urban land surface temperature.

With continuing economic and social development, the number of urban buildings continues to increase, and human activities have altered the characteristics of the urban land surface, resulting in an intensified UHI effect, which will inevitably have a negative effect on the urban microclimate. The characteristics of the urban thermal environment are closely related to human thermal comfort. Existing studies have proved that natural parameters like air temperature and humidity, wind speed, solar radiation, soil temperature, and humidity are very sensitive to any three-dimensional changes in an urban setting. Urban geometry has a significant influence on urban microclimate conditions (Omar, David, & Hatem, 2020; Tania, Koen, & Andreas, 2017). Four of these meteorological parameters, namely temperature, relative humidity, mean radiation temperature, and wind speed, are directly affected by urban morphology and surface materials. They are all closely related to land surface temperature and the thermal environment and are the most important climatic parameters that affect thermal comfort (Cao, Zhou, Zheng, Ren, & Wang, 2021; Goldblatt, Addas, Crull, Maghrabi, & Levin, 2021; Nasrollahi, Ghosouri, Khodakarami, & Taleghani, 2020; Tsoka et al., 2018a, 2018b; Yang, Shi et al., 2020; Yang, Wang et al., 2020). As the main characterization factor of the urban thermal environment, excessively high land surface temperatures will ultimately lead to thermal discomfort in cities, which is not conducive to the thermal experience of urban residents (Goldblatt et al., 2021; Nasrollahi et al., 2020; Obiefuna, Okolie, Nwilo, Daramola, & Isiofia, 2021). Therefore, it is necessary to understand the formation and variation of the urban thermal environment by determining which indicator has the greatest impact on LST and then exploring how the four thermal environment representational variables are affected by different building densities.

4.2. Correlation analysis results

The correlations calculated between the surface temperature and its influencing factors exhibited significant variation at different grid scales and study sites. For example, at a grid scale of 30 m, the correlation between building density and land surface temperature in Dalian in 2002 and 2014 was 0.514 and 0.537, respectively (Su et al., 2018), while the correlation between building height and land surface temperature in 2007 and 2017 was 0.346 and 0.331, respectively (Yan et al., 2019). However, in Chongqing (which is a mountainous city), under the same spatial scale of 30 m, the correlation between building density and land surface temperature was only 0.047. Moreover, PR does not show a significant correlation with land surface temperature (Guo et al., 2020). When examining the correlation between SVF and land surface temperature, Guo et al. (2020) found that as grid size increases, the correlation coefficient increases and is always positive; however, Chun and Guldmann (2014) showed that the smaller the grid scale, the weaker the explanatory effect of SVF on land surface temperature, and that the correlation coefficient was always negative. Therefore, different study sites and scales will influence the calculation results (Berger et al., 2017; Chun & Guldmann, 2014; Guo et al., 2020; Scarano & Mancini, 2017). This study used a grid scale of 100 m to remain consistent with the scale of the simulation, so that the correlation coefficient could be calculated. The resulting correlation coefficients between land surface temperature and FAR, PR, Ra, λc, and SVF were 0.569, 0.446, 0.429, 0.463, and -0.270, respectively, indicating that the optimal scale of the correlation analysis should be determined according to the specific morphological indicators and the study site.

4.3. ENVI-met simulation

In this study, the data from the meteorological station were used as the initial conditions; PE, RMSE, and R^2 were used to evaluate the

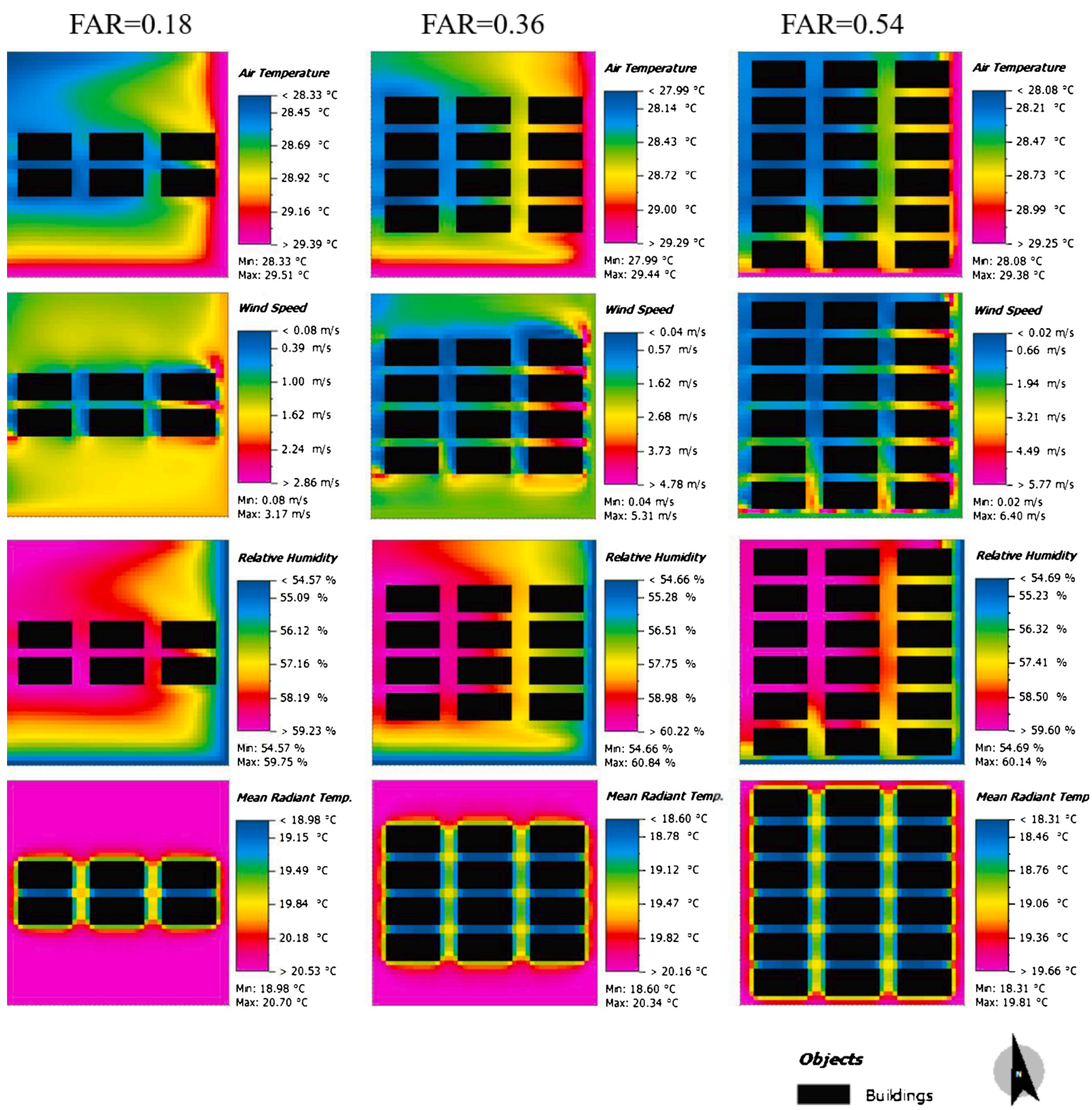

Fig. 7. Visualization results of air temperature, wind speed, relative humidity and mean radiation temperature for three models at 14:00.

accuracy of the simulation. The evaluation results were as follows: temperature exhibited a minimum PE of 1.26 %, maximum PE of 6.29 %, and average statistical error of 3.90 %, with RMSE of 1.23 °C, and R^2 of 0.870. Compared with the accuracy range of other studies, the overall value is within the range of acceptable error (PE = 3.75 %, RMSE = 1.11–1.62 °C, R^2 >0.80) (Chen, Wu, Yu, & Wang, 2020; Wang et al., 2018; Yang, Shi et al., 2020; Yang, Wang et al., 2020), indicating that the simulation results are relatively reliable.

As a micro-scale model, ENVI-met is an important tool for urban climate analysis. Most of the existing research has focused on the scale of a community or block, generally within 500 m, and the simulation results have been proved to be relatively scientific and reliable (Dario, Giorgio, Biagio, Iole, & Stefano, 2014; P López-Cabeza, Galán-Marín, Rivera-Gómez, & Roa-Fernández, 2018; Tsoka et al., 2018a, 2018b). Therefore, this study simplified the modeling of small-scale buildings, aiming to simulate the impact of changing building density on the surrounding thermal environment, and study the variation in the thermal environment on a micro scale, to further reflect on the urban scale. The results showed that even in a small area, the urban microclimate showed significant variation. Therefore, we have reason to believe that changes in building density will inevitably lead to changes in the thermal environment on a larger urban scale. Determining the relationship between regional microclimate characteristics and building density, based on ENVI-met simulations, is helpful for the optimization of urban residential planning and design, and provides a basis for environmental improvement of built-up areas. Due to the limitation of scale and other problems, the simulation results cannot accurately reflect specific impacts of building density changes on the urban environment, but it still provides the overall variation trend of the thermal environment. However, future studies should consider the scale of the research and explore the scientific relationship between building density and wind speed in real urban spaces.

4.4. Limitations

There are many limitations to this study, including the lack of a standard reference scale for the grid division of the study area, which may affect the accuracy of the calculated urban morphological indicators and the correlations between the indicators and land surface temperature. In numerical simulations, data from the meteorological stations were used directly as the initial conditions, the urban building model and layout were simplified without considering objective factors

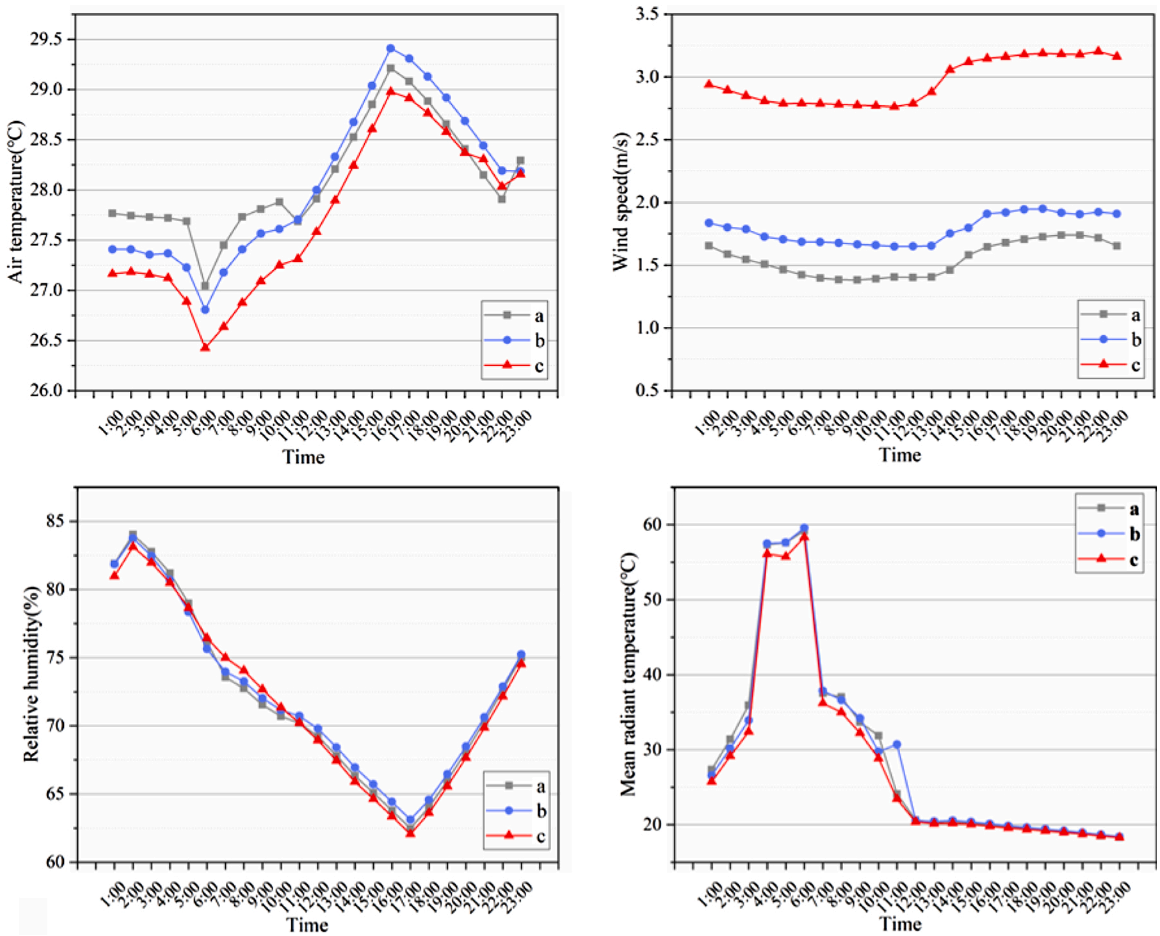

Fig. 8. 24-h change curves of air temperature, wind speed, relative humidity and mean radiation temperature(a, b and c represent FAR of 0.18,0.36 and 0.54, respectively).

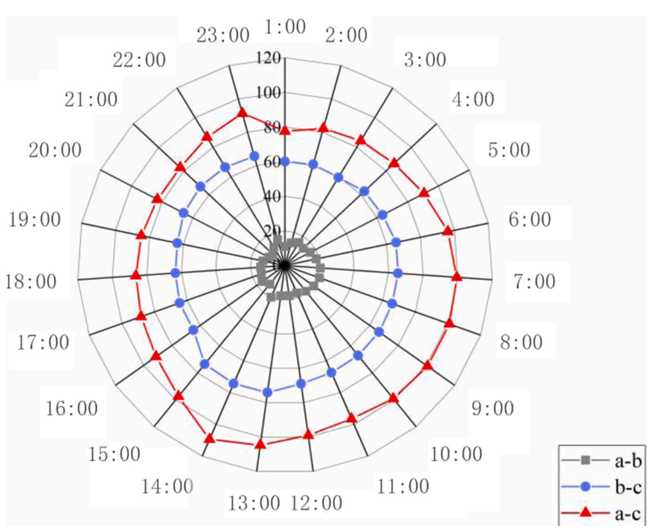

Fig. 9. 24 h wind speed change rate(%)(a, b and c represent FAR of 0.18,0.36 and 0.54, respectively).

such as building materials and vegetation, which means that the cooling effect of vegetation was ignored, which may impact the simulation results. Therefore, the role of vegetation in reducing the UHI effect should be considered in future research, and changes to the thermal environment within urban spaces should be discussed by integrating the vegetation distribution and three-dimensional characteristics of the city.

5. Conclusions

In this study, Landsat-8 OLI remote sensing data was used to obtain the urban surface temperature of Dalian, China; a series of urban morphology indicators were selected and calculated to study the relationship between the thermal environment and the three-dimensional building morphology in Dalian's central urban area. Furthermore, the numerical simulation software ENVI-met was used to simulate the thermal environment of the study area to determine the effects of architectural morphology on the surrounding thermal environment. The results can be summarized as follows:

(1) The land surface temperature of the study area ranged from 23.2–50.7 °C, and the global spatial autocorrelation coefficient (Moran's I) was 0.94, indicating that land surface temperature exhibits a strong positive spatial correlation. The FAR ranged from 0.2 to 0.6, PR ranged from 2 to 6, and SVF ranged from 0 to 0.4, demonstrating that the buildings in the study area are mainly multi-story and high-rise buildings and primarily distributed within a medium-density area. The high-density and high-rise buildings are mostly distributed in the financial and commercial center of the research area, which conforms to the reality that high-rise buildings have become common in cities due to the continuous increase in urban construction and continuous decrease in available urban land associated with rapid economic and social development.

(2) The correlation coefficients between the land surface temperature and FAR, PR, Ra, λc, and SVF were calculated as 0.569, 0.446, 0.429, 0.463, and −0.270, respectively. In other words, building density has the greatest influence on and is positively correlated with the land surface temperature, whereas SVF has the smallest influence and is negatively correlated with the land surface temperature.
(3) Building density mainly affects the urban thermal environment by influencing the wind speed. In medium density (FAR < 0.6) areas, there is a positive correlation between wind speed and building density. As the building density increases, the wind speed increases. However, wind speed is also affected by building height, building materials and other aspects, thus influencing the land surface temperature. Therefore, under the premise of fixed building density, measures such as increasing building height, changing building materials, and planning building layout to construct reasonable ventilation corridors can improve urban ventilation and reduce the UHI effect.

By combining correlation analysis and numerical simulations, this study analyzed the relationship between three-dimensional morphological characteristics and the local thermal environment in Dalian, China. This study, therefore, improves our understanding how the three-dimensional morphology impacts the urban thermal environment and can provide scientific suggestions for future urban planning and construction, thereby effectively alleviating the UHI effect and realizing sustainable urban development.

Declaration of Competing Interest

This manuscript has not been published or presented elsewhere in part or in entirety and is not under consideration by another journal. We have read and understood your journal's policies, and we believe that neither the manuscript nor the study violates any of these. There are no conflicts of interest to declare.

Acknowledgements

The authors would like to acknowledge all colleagues and friends who have voluntarily reviewed the translation of the survey and the manuscript of this study. This research study was supported by the National Natural Science Foundation of China (grant no. 41771178, 42030409, 41671151), the Fundamental Research Funds for the Central Universities (grant no. N2111003), the Second Tibetan Plateau Scientific Expedition and Research Program (STEP) (grant no. 2019QZKK1004), and Innovative Talents Support Program of Liaoning Province (Grant No. LR2017017).

References

Abdallah, A. S. H., Hussein, S. W., & Nayel, M. (2020). The impact of outdoor shading strategies on student thermal comfort in open spaces between education building. *Sustainable Cities and Society, 58*, Article 102124. https://doi.org/10.1016/j.scs.2020.102124

Allegrini, J., Dorer, V., & Carmeliet, J. (2015). Influence of morphologies on the microclimate in urban neighborhoods. *Journal of Wind Engineering and Industrial Aerodynamics, 144*, 108–117. https://doi.org/10.1016/j.jweia.2015.03.024

Antonio, L., Federica, G., Raffaele, P., & Francesca, C. (2020). Nature-based climate adaptation for compact cities: Green courtyards as urban cool islands. *Plurimondi, 18*, 83–110. http://plurimondi.poliba.it/index.php/Plurimondi/article/view/156.

Antoniou, N., Montazeri, H., Neophytou, M., & Blocken, B. (2019). CFD simulation of urban microclimate: Validation using high-resolution field measurements. *The Science of the Total Environment, 695*, Article 133743. https://doi.org/10.1016/j.scitotenv.2019.133743

Berger, C., Rosentreter, J., Voltersen, M., Baumgart, C., Schmullius, C., et al. (2017). Spatio-temporal analysis of the relationship between 2D/3D urban site characteristics and land surface temperature. *Remote Sensing of Environment, 193*, 225–243. https://doi.org/10.1016/j.rse.2017.02.020

C40 China Buildings Programme (C40 CBP). (2018). *Constructing a New Low Carbon Future: How Chinese cities are scaling ambitious building energy efficiency solutions*. Retrieved from https://c40-production-images.s3.amazonaws.com/res-earches/images/72_C40_China_Buildings_Programme_Launch_Report_-_English_Layout_Web.original.pdf?1538030392.

C40 cities. (2018). *Urban climate action impacts framework: A framework describing and measuring the wider impacts of urban climate action*. Retrieved from https://c40-production-images.s3.amazonaws.com/other_uploads/images/1670_C-40_UCAIF_report_26_Feb_2.original.pdf?1521042661.

Cao, J., Zhou, W., Zheng, Z., Ren, T., & Wang, W. (2021). Within-city spatial and temporal heterogeneity of air temperature and its relationship with land surface temperature. *Landscape and Urban Planning, 206*, Article 103979. https://doi.org/10.1016/j.landurbplan.2020.103979

Chen, Y., Wu, J., Yu, K., & Wang, D. (2020). Evaluating the impact of the building density and height on the block surface temperature. *Building and Environment, 168*, Article 106493. https://doi.org/10.1016/j.buildenv.2019.106493

China MOCP. (2015). *Code for design of civil buildings. GB 50352-52005*. Retrieved from. China Architecture & Building Press https://www.soujianzhu.cn/Norm/JzzyXq.aspx?id=386.

Chun, B., & Guldmann, J. M. (2014). Spatial statistical analysis and simulation of the urban heat island in high-density central cities. *Landscape and Urban Planning, 125*, 76–88. https://doi.org/10.1016/j.landurbplan.2014.01.016

Dario, A., Giorgio, G., Biagio, M., Iole, N., & Stefano, S. (2014). Evaluating mitigation effects of urban heat islands in a historical small center with the ENVI-Met® climate model. *Sustainability, 6*, 7013–7029. https://doi.org/10.3390/su6107013

Fan, P., Yue, W., Zhang, J., Huang, H., Messina, J., et al. (2020). The spatial restructuring and determinants of industrial landscape in a mega city under rapid urbanization. *Habitat International, 95*, Article 102099. https://doi.org/10.1016/j.habitatint.2019.102099

Farshid, A., Ester, H. G., Ebrahim, S., & Soran, M. (2019). Urban green space cooling effect in cities. *Heliyon, 5*, 1339. https://doi.org/10.1016/j.heliyon.2019.e01339

Feng, Z., Wang, S., Jin, S., & Yang, J. (2019). The influence of urban morphology and wind environment on surface temperature in Changchun city. *Journal of Geographical Sciences, 74*, 902–911. http://kns.cnki.net/KCMS/detail/detail.aspx?FileName=DLXB201905006&DbName=CJFQ2019.

Galal, O. M., Sailor, D. J., & Mahmoud, H. (2020). The impact of urban form on outdoor thermal comfort in hot arid environments during daylight hours, case study: New Aswan. *Building and Environmnet, 184*, 107222. https://doi.org/10.1016/j.buildenv.2020.107222

Goldblatt, R., Addas, A., Crull, D., Maghrabi, A., Levin, G. G., et al. (2021). Remotely sensed derived land surface temperature (LST) as a proxy for air temperature and thermal comfort at a small geographical scale. *Land, 10*, 410. https://doi.org/10.3390/land10040410.Guo

Guo, J., Han, G., Xie, Y., Cai, Z., & Zhao, Y. (2020). Exploring the relationships between urban spatial form factors and land surface temperature in mountainous area: A case study in Chongqing city, China. *Sustainable Cities and Society, 61*, Article 102286. https://doi.org/10.1016/j.scs.2020.102286

He, B. (2019). Towards the next generation of green building for urban heat island mitigation: Zero UHI impact building. *Sustainable Cities and Society, 50*, Article 101647. https://doi.org/10.1016/j.scs.2019.101647

He, B., Ding, L., & Prasad, D. (2020a). Relationships among local-scale urban morphology, urban ventilation, urban heat island and outdoor thermal comfort under sea breeze influence. *Sustainable Cities and Society, 60*, Article 102289. https://doi.org/10.1016/j.scs.2020.102289

He, B., Ding, L., & Prasad, D. (2020b). Wind-sensitive urban planning and design: Precinct ventilation performance and its potential for local warming mitigation in an open midrise gridiron precinct. *Journal of Building Engineering, 29*. https://doi.org/10.1016/j.jobe.2019.101145

Huang, J., & Chen, L. (2020). A numerical study on mitigation strategies of urban heat islands in a tropical megacity: A case study in Kaohsiung City, Taiwan. *Sustainability (Basel, Switzerland), 12*, 3952. https://doi.org/10.3390/su12103952

Huang, C., Tsai, H., & Chen, H. (2020). Influence of weather factors on thermal comfort in subtropical urban environments. *Sustainability (Basel, Switzerland), 12*(2001). https://doi.org/10.3390/su12052001

Jiang, S., Zhan, W., Yang, J., Liu, Z., & Huang, F. (2020). Research progress on spatiotemporal differentiation of urban heat island under the framework of local climate zoning. *Journal of Geographical Sciences, 75*, 1860–1878. http://kns.cnki.net/KCMS/detail/detail.aspx?FileName=DLXB202009005&DbName=DKFXTEMP.

Kibria, K. R., Timothy, O., Jedediah, B. A., & OhJin, W. (2016). Simulating the effects of cool roof and PCM (phase change materials) based roof to mitigate UHI (urban heat island) in prominent US cities. *Energy, 96*, 103–117. https://doi.org/10.1016/j.energy.2015.11.082

Ku, C., & Tsai, H. (2020). Evaluating the influence of urban morphology on urban wind environment based on computational fluid dynamics simulation. *ISPRS International Journal of Geo-Information, 9*, 399. https://doi.org/10.3390/ijgi9060399

Kuang, W. (2018). Research progress and prospect of urban land use/cover change and ecological regulation of thermal environment. *Scientia Geographica Sinica, 38*, 1643–1652. http://kns.cnki.net/KCMS/detail/detail.aspx?FileName=DLKX201810008&DbName=DKFX2018.

Li, G., Ren, Z., & Zhan, C. (2020). Sky View Factor-based correlation of landscape morphology and the thermal environment of street canyons: A case study of Harbin, China. *Building and Environmnet, 169*, Article 106587. https://doi.org/10.1016/j.buildenv.2019.106587

Liu, Y., Li, Q., Yang, L., Mu, K., Zhang, M., et al. (2020). Urban heat island effects of various urban morphologies under regional climate conditions. *The Science of the Total Environment, 743*, Article 140589. https://doi.org/10.1016/j.scitotenv.2020.140589

Luo, X., Yang, J., Sun, W., & He, B. (2021). Suitability of human settlements in mountainous areas from the perspective of ventilation: A case study of the main urban area of Chongqing. *Journal of Cleaner Production, 310*, Article 127467. https://doi.org/10.1016/j.jclepro.2021.127467

Mahanta, N. R., & Samuel, A. K. (2020). Study of land surface temperature (LST) and land cover for urban heat island (UHI) analysis in Dubai. *2020 8th International Conference on Reliability, Infocom Technologies and Optimization (Trends and Future Directions) (ICRITO)*, 1285–1288. https://doi.org/10.1109/ICRITO48877.2020.9198038

McKinsey. (2017). *Focused acceleration: A strategic approach to climate action in cities to 2030*. Retrieved from https://www.c40.org/researches/mckinsey-center-for-business-and-environment.

Meng, F., & Xiao, Q. (2018). Landsat 8 image-based analysis of the urban heat island characteristics in Jinan, China. *IEEE International Geoscience and Remote Sensing Symposium*, 2976–2979. https://doi.org/10.1109/IGARSS.2018.8517305

Nasrollahi, N., Ghosouri, A., Khodakarami, J., & Taleghani, M. (2020). Heat-mitigation strategies to improve pedestrian thermal comfort in urban environments: A review. *Sustainability, 12*, 10000. https://doi.org/10.3390/su122310000

Obiefuna, J. N., Okolie, C. J., Nwilo, P. C., Daramola, O. E., & Isiofia, L. C. (2021). Potential influence of urban sprawl and changing land surface temperature on outdoor thermal comfort in Lagos State, Nigeria. *Quaestiones Geographicae, 40*. https://doi.org/10.2478/quageo-2021-0001

Omar, M. G., David, J. S., & Hatem, M. (2020). The impact of urban form on outdoor thermal comfort in hot arid environments during daylight hours, case study: New Aswan. *Building and Environment, 184*, Article 107222. https://doi.org/10.1016/j.buildenv.2020.107222

P López-Cabeza, C. V., Galán-Marín, C., Rivera-Gómez, C., & Roa-Fernández, J. (2018). Courtyard microclimate ENVI-met outputs deviation from the experimental data. *Building and Environmnet, 144*, 129–141. https://doi.org/10.1016/j.buildenv.2018.08.013

Qiao, Z., Huang, N., Xu, X., Sun, Z., Wu, C., et al. (2019). Temporal and spatial differentiation characteristics and evolution rules of surface thermal landscape in Beijing from 2003 to 2017. *Journal of Geographical Sciences, 74*, 475–489. http://kns.cnki.net/KCMS/detail/detail.aspx?FileName=DLXB201903007&DbName=CJFQ2019.

Qiao, Z., Sun, Z., Sun, X., Xu, X., & Yang, J. (2019). Urban thermal environment risk prediction and spatial and temporal pattern analysis. *Acta Ecologica Sinica, 39*, 649–659. http://kns.cnki.net/KCMS/detail/detail.aspx?FileName=STXB201902026&DbName=CJFQ2019.

Qin, Z., Zhang, M., Karnieli, A., & Berliner, P. (2001). Mono-window algorithm for retrieving land surface temperature from Landsat TM6 data. *Acta Geographica Sinica, 68*, 456–466. http://www.wanfangdata.com.cn/details/detail.do?_type=perio&id=dlxb200104009.

Ren, C., Cai, M., Li, X., Shi, Y., & Linda, S. (2020). Developing a rapid method for 3-dimensional urban morphology extraction using open-source data. *Sustainable Cities and Society, 53*. https://doi.org/10.1016/j.scs.2019.101962

Ren, C., Yang, R., Cheng, C., Xing, P., Fang, X., et al. (2018). Creating breathing cities by adopting urban ventilation assessment and wind corridor plan – The implementation in Chinese cities. *Journal of Wind Engineering and Industrial Aerodynamisc, 182*, 170–188. https://doi.org/10.1016/j.jweia.2018.09.023

Salata, F., Golasi, I., Vollaro, A. D. L., & Vollaro, R. D. L. (2015). How high albedo and traditional buildings' materials and vegetation affect the quality of urban microclimate. A case study. *Energy and Buildings, 99*, 32–49. https://doi.org/10.1016/j.enbuild.2015.04.010

Santamouris, M., & Young Yun, G. (2020). Recent development and research priorities on cool and super cool materials to mitigate urban heat island. *Renewable Energy, 161*, 792–807. https://doi.org/10.1016/j.renene.2020.07.109

Scarano, M., & Mancini, F. (2017). Assessing the relationship between sky view factor and land surface temperature to the spatial resolution. *International Journal of Remote Sensing, 38*, 6910–6929. https://doi.org/10.1080/01431161.2017.1368099

Sharmin, T., Steemers, K., & Matzarakis, A. (2017). Microclimatic modelling in assessing the impact of urban geometry on urban thermal environment. *Sustainable Cities and Society, 34*, 293–308. https://doi.org/10.1016/j.scs.2017.07.006

Stewart, I. D., & Oke, T. R. (2012). Local climate zones for urban temperature studies. *Bulletin of the American Meteorological Society, 93*, 1879–1900. https://doi.org/10.1175/BAMS-D-11-00019.1

Stewart, I. D., Oke, T. R., & Krayenhoff, E. S. (2014). Evaluation of the 'local climate zone' scheme using temperature observations and model simulations. *International Journal of Climatology, 34*, 1062–1080. https://doi.org/10.1002/joc.3746

Su, J., Lv, F., & Yang, J. (2018). The Influence of urban building Level characteristics on urban thermal environmental effect - A case study of Zhongshan District in Dalian. *Bulletin of Surveying and Mapping*, 111–114. http://kns.cnki.net/KCMS/detail/detail.aspx?FileName=CHTB201808023&DbName=CJFQ2018.

Sun, F., Liu, M., Wang, Y., Wang, H., & Che, Y. (2020). The effects of 3D architectural patterns on the urban surface temperature at a neighborhood scale: Relative contributions and marginal effects. *Journal of Cleaner Production, 258*, Article 120706. https://doi.org/10.1016/j.jclepro.2020.120706

Tania, S., Koen, S., & Andreas, M. (2017). Microclimatic modelling in assessing the impact of urban geometry on urban thermal environment. *Sustainable Cities and Society, 34*, 293–308. https://doi.org/10.1016/j.scs.2017.07.006

Tian, Y., Zhou, W., Qian, Y., Zheng, Z., & Yan, J. (2019). The effect of urban 2D and 3D morphology on air temperature in residential neighborhoods. *Landscape Ecology, 34*, 1161–1178. https://doi.org/10.1007/s10980-019-00834-7

Toparlar, Y., Blocken, B., Maiheu, B., & van Heijst, G. J. F. (2017). A review on the CFD analysis of urban microclimate. *Renewable and Sustainable Energy Reviews, 80*, 1613–1640. https://doi.org/10.1016/j.rser.2017.05.248

Tsoka, S., Tsikaloudaki, A., & Theodosiou, T. (2018a). Analyzing the ENVI-met microclimate model's performance and assessing cool materials and urban vegetation applications–A review. *Sustainable Cities and Society, 43*, 55–76. https://doi.org/10.1016/j.scs.2018.08.009

Tsoka, S., Tsikaloudaki, A., & Theodosiou, T. (2018b). Analyzing the ENVI-met microclimate model's performance and assessing cool materials and urban vegetation applications–A review. *Sustainable Cities and Society, 43*, 55–76. https://doi.org/10.1016/j.scs.2018.08.009

Wang, Y., Zhou, D., Wang, Y., Fang, Y., Yuan, Y., et al. (2018). Comparative study of urban residential design and microclimate characteristics based on ENVI-met simulation. *Indoor and Built Environment, 28*, 1200–1216. https://doi.org/10.1177/1420326X19860884

Wang, B., Cot, L. D., Adolphe, L., Geoffroy, S., & Sun, S. (2017). Cross indicator analysis between wind energy potential and urban morphology. *Renewable Energy, 113*, 989–1006. https://doi.org/10.1016/j.renene.2017.06.057

Wang, W., Liang, H., Yang, L., Liu, K., Su, H., et al. (2017). Analyzing the urban heat island using time series land surface temperature (LST) data. *IEEE International Geoscience and Remote Sensing Symposium (IGARSS)*, 5874–5876. https://doi.org/10.1109/IGARSS.2017.8128345

Wei, R., Song, D., Wong, N. H., & Martin, M. (2016). Impact of urban morphology parameters on microclimate. *Procedia Engineering, 169*, 142–149. https://doi.org/10.1016/j.proeng.2016.10.017

Yan, G., Su, J., & Guan, D. (2019). Influence of vertical characteristics of urban buildings on urban thermal environmental effect in the middle mountainous area of Dalian city. *Scientia Geographica Sinica, 39*, 125–130. http://kns.cnki.net/KCMS/detail/detail.aspx?FileName=DLKX201901014&DbName=DKFX2019.

Yang, J., Sun, J., Ge, Q., & Li, X. (2017). Assessing the impacts of urbanization-associated green space on urban land surface temperature: A case study of Dalian, China. *Urban Forestry & Urban Greening, 22*, 1–10. https://doi.org/10.1016/j.ufug.2017.01.002

Yang, J., Su, J., Xia, J., Jin, C., Li, X., et al. (2018). The impact of spatial form of urban architecture on the urban thermal environment: A case study of the Zhongshan District, Dalian, China. *IEEE Journal of Selected Topics in Applied Earth Observations and Remote Sensing, 11*, 2709–2716. https://doi.org/10.1109/JSTARS.2018.2808469

Yang, L., Niyogi, D., Tewari, M., Aliaga, D., Chen, F., et al. (2016). Contrasting impacts of urban forms on the future thermal environment: Example of Beijing metropolitan area. *Environmental Research Letters, 11*, 34018. https://doi.org/10.1088/1748-9326/11/3/034018

Yang, J., Jin, S., Xiao, X., Jin, C., Xia, J. C., et al. (2019). Local climate zone ventilation and urban land surface temperatures: Towards a performance-based and wind-sensitive planning proposal in megacities. *Sustainable Cities and Society, 47*, Article 101487. https://doi.org/10.1016/j.scs.2019.101487

Yang, J., Ren, J., Sun, D., Xiao, X., Xia, J. C., et al. (2021). Understanding land surface temperature impact factors based on local climate zones. *Sustainable Cities and Society, 69*, Article 102818. https://doi.org/10.1016/j.scs.2021.102818

Yang, J., Shi, B., Xia, G., Xue, Q., & Cao, S. (2020). Impacts of urban form on thermal environment near the Surface Region at pedestrian height: A case study based on high-density built-up areas of Nanjing City in China. *Sustainability (Basel, Switzerland), 12*, 1737. https://doi.org/10.3390/su12051737

Yang, J., Wang, Y., Xiu, C., Xiao, X., Xia, J., et al. (2020). Optimizing local climate zones to mitigate urban heat island effect in human settlements. *Journal of Cleaner Production, 275*, Article 123767. https://doi.org/10.1016/j.jclepro.2020.123767

Yang, J., Wang, Y., Xiao, X., Jin, C., Xia, J. C., et al. (2019). Spatial differentiation of urban wind and thermal environment in different grid sizes. *Urban Climate, 28*, Article 100458. https://doi.org/10.1016/j.uclim.2019.100458

Yao, Y., Chen, X., & Qian, J. (2018). Research progress of urban surface thermal environment. *Acta Ecologica Sinica, 38*, 1134–1147. http://kns.cnki.net/KCMS/detail/detail.aspx?FileName=STXB201803038&DbName=CJFQ2018.

Yu, Z., Chen, S., & Wong, N. H. (2020). Temporal variation in the impact of urban morphology on outdoor air temperature in the tropics: A campus case study. *Building and Environment, 181*, Article 107132. https://doi.org/10.1016/j.buildenv.2020.107132

Yue, W., Liu, X., Zhou, Y., & Liu, Y. (2019). Impacts of urban configuration on urban heat island: An empirical study in China mega-cities. *The Science of the Total Environment, 671*, 1036–1046. https://doi.org/10.1016/j.scitotenv.2019.03.421

Yue, W., Zhang, L., & Liu, Y. (2016). Measuring sprawl in large Chinese cities along the Yangtze River via combined single and multidimensional metrics. *Habitat International, 57*, 43–52. https://doi.org/10.1016/j.habitatint.2016.06.009

Zhai, P., Yuan, Y., Yu, R., & Guo, J. (2019). Climate change and sustainable urban development. *Chinese Science Bulletin, 64*, 1995–2001. http://kns.cnki.net/KCMS/detail/detail.aspx?FileName=KXTB201919004&DbName=CJFQ2019.

Zhang, Y., & Cheng, J. (2019). Spatio-temporal analysis of urban heat island using multisource remote sensing data: A case study in Hangzhou, China. *IEEE Journal of Selected Topics in Applied Earth Observations and Remote Sensing, 12*, 3317–3326. https://doi.org/10.1109/jstars.2019.2926417

Zhang, A., Li, W., Wu, J., Lin, J., Chu, J., et al. (2020). How can the urban landscape affect urban vitality at the street block level? A case study of 15 metropolises in China. *Environment and Planning B, Urban Analytics and City Science*. https://doi.org/10.1177/2399808320924425, 239980832092442.

Zhao, Z., Shen, L., Li, L., Wang, H., & He, B. (2020). Local climate zone classification scheme can also indicate local-scale urban ventilation performance: An evidence-based study. *Atmosphere, 11*, 776. https://doi.org/10.3390/atmos11080776

Zhou, W., & Tian, Y. (2020). Research progress in the thermal environmental effects of three-dimensional urban spatial morphology. *Acta Ecologica Sinica, 40*, 416–427. http://kns.cnki.net/KCMS/detail/detail.aspx?FileName=STXB202002003&DbName=CJFQ2020.